

## FRET analysis with Pulsed Interleaved Excitation (PIE) using the MicroTime 200

Steffen Ruettinger, Volker Buschmann, Benedikt Kraemer, Sandra Orthaus, Felix Koberling

PicoQuant GmbH, Rudower Chaussee 29, 12489 Berlin, Germany, [info@picoquant.com](mailto:info@picoquant.com)

### Introduction

Förster Resonance Energy Transfer (FRET) describes a process in which energy from an excited molecule (Donor) is transferred to a second molecule (Acceptor), which may fluoresce. As the amount of energy transferred is sensitive to the distance between these two molecules, this technique is used to measure intra- and intermolecular distances on a nanometer scale and has consequently found a broad range of applications, e.g., in binding studies and protein folding investigations [1-3]. However, the analysis of FRET measurements is often complicated by the fact that not all molecules under study are necessarily marked with both donor and acceptor molecule, but often lack e.g., the acceptor molecule. Additional complications arise from multiple labeled species giving not only one but multiple FRET processes. A differentiation between these single species is therefore desirable, but effectively only possible on the single molecule level.

One approach is based on the Pulsed Interleaved Excitation (PIE) [4] or Alternating Laser Excitation (ALEX) [5,6] of both, the acceptor and the donor molecule. Briefly, PIE or ALEX<sup>1</sup> [7] is used to excite the acceptor dye independently of the FRET process and to prove its existence via fluorescence.

<sup>1</sup> Historically, the difference between PIE and ALEX was that for ALEX CW lasers were interleaved on the  $\mu\text{s}$  time scale as opposed to interleaved ps laser pulses. Later, the term ns ALEX has been introduced to highlight the interleaving of pulsed lasers on the ns time scale. In this application note, the term PIE will be used; we treat PIE and ns ALEX as synonyms.

This technique allows to differentiate a FRET molecule, even with a very low FRET efficiency from a molecule with an absent or non-fluorescing acceptor. Such incomplete FRET molecules lead to a zero efficiency peak [1] in the FRET efficiency histogram.

Building on the interleaved excitation of donor and acceptor, different Multi-Parameter Detection (MFD) [8] schemes have been developed to further enhance the amount of information that can be gained. MFD enables a robust FRET analysis, possible artifacts originating from e.g., quenching or photobleaching are identified and can be separated from the FRET species.

This application note describes the use of the confocal fluorescence microscope MicroTime 200 [9] for single molecule FRET studies employing PIE and MFD. Three examples will be showcased:

- The first deals with the working horse of FRET experiments, the polyproline molecule. We will show how PIE effectively enables suppressing the infamous zero efficiency peak.
- Secondly, building on the additional information conveyed by PIE, we are able to plot the labeling stoichiometry together with the FRET, select subpopulations and leveraging the fluorescence lifetime, determine the FRET efficiencies of those subpopulations without the need for calibration measurements.
- Finally, we show that using MFD the donor-acceptor intensity ratio can be plotted against the burst integrated lifetime into a 2D-histogram.

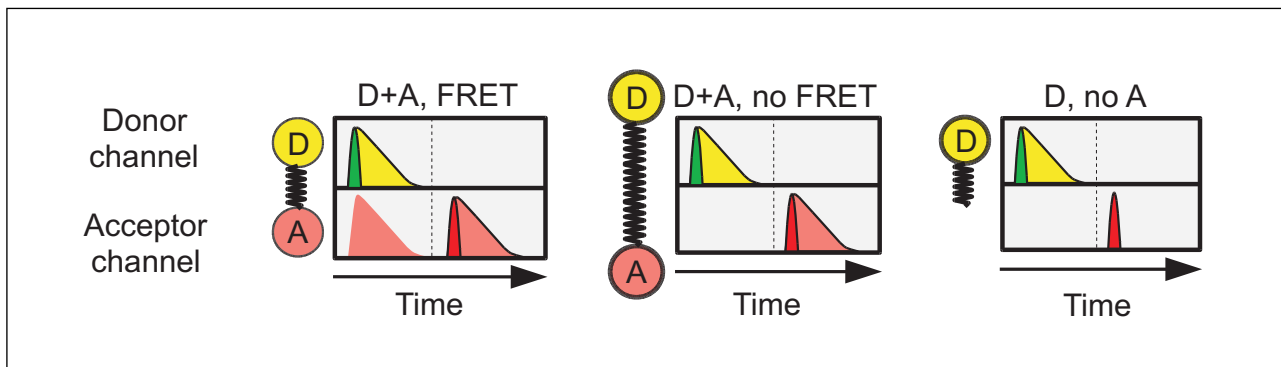


Fig. 1: Schematic PIE-FRET results for a close FRET pair (left), a well separated FRET pair (middle) and a donor molecule lacking a FRET acceptor (right).

By comparing the resulting distribution with the theoretically expected dependence, one can assess various parameters such as spectral bleed-through.

through) and to eliminate the zero efficiency peak.

## Principle of PIE-FRET

PIE-FRET can be used to identify FRET molecules with a non-fluorescing or absent acceptor molecule. Two lasers are chosen with suitable wavelengths for the excitation of both, the donor and acceptor molecule. The laser pulses are delayed with respect to each other to yield a pulse sequence with interleaved pulses. In our set-up, the fluorescence after excitation with the green laser is visible in the early time window and that of the red laser in the late time window (see Fig. 1). Each diagram shows in the upper part the fluorescence decay measured in the donor detection channel and in the lower part the decay detected in the acceptor channel along with a schematic representation of the laser pulse.

## PIE-FRET eliminates the zero efficiency peak in FRET histograms

Polyproline peptides have been established as reference molecules for FRET, both in ensemble [10] and single molecule experiments [11]. In the following, results are shown for a peptide containing 12 polyproline residues. N-terminal glycine and C-terminal cysteine were attached to permit labeling of opposite ends with Alexa Fluor 647 and Alexa Fluor 555 (Molecular Probes, Eugene, USA) as acceptor and donor fluorophores (Alexa Fluor 647-Gly-(Pro)<sub>12</sub>-Cys-maleimide-Alexa Fluor 555). The length of the polyproline 12 spacer accounts to around 4 nm, a value near the calculated Förster radius of 5 nm [12] of the FRET pair. Fig. 2 shows a molecular model of a FRET pair with a polyproline 12 spacer and two Alexa Fluor dyes.

The left and middle pane of Fig. 1 schematically show the complete FRET pairs under study: Excitation with the red laser only leads to observable fluorescence from the acceptor molecule in the late time window while on the other hand, excitation of the donor molecule with the green laser results in fluorescence from the donor as well as from the acceptor molecule due to FRET in the early time window. If the distance between the donor and the acceptor molecule is too large for an efficient FRET process, like schematically shown in the middle of Fig. 1, one only observes fluorescence from each excited fluorophore after direct excitation. Finally, molecules lacking the acceptor molecule (Fig. 1, right), consequently show no emission at all after red excitation in the late time window. In that way, incomplete FRET molecules without a fluorescing acceptor (or donor fluorophore respectively) are identified. The resulting information can be used for the calculation of correction parameters (e.g. for direct excitation or bleed

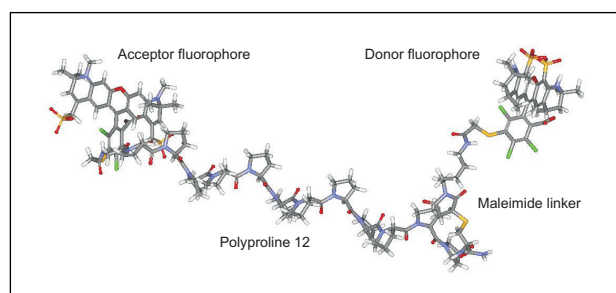


Fig. 2: Molecular model of a peptide containing 12 proline residues and maleimide linker with the donor and acceptor dyes Alexa Fluor 555 and Alexa Fluor 647.

## Experimental details

The acceptor was excited with a picosecond pulsed diode laser at 638 nm whereas the donor molecule was excited using a PicoTA laser emitting at 532 nm. Narrow band clean-up filters ensured that no parasitic

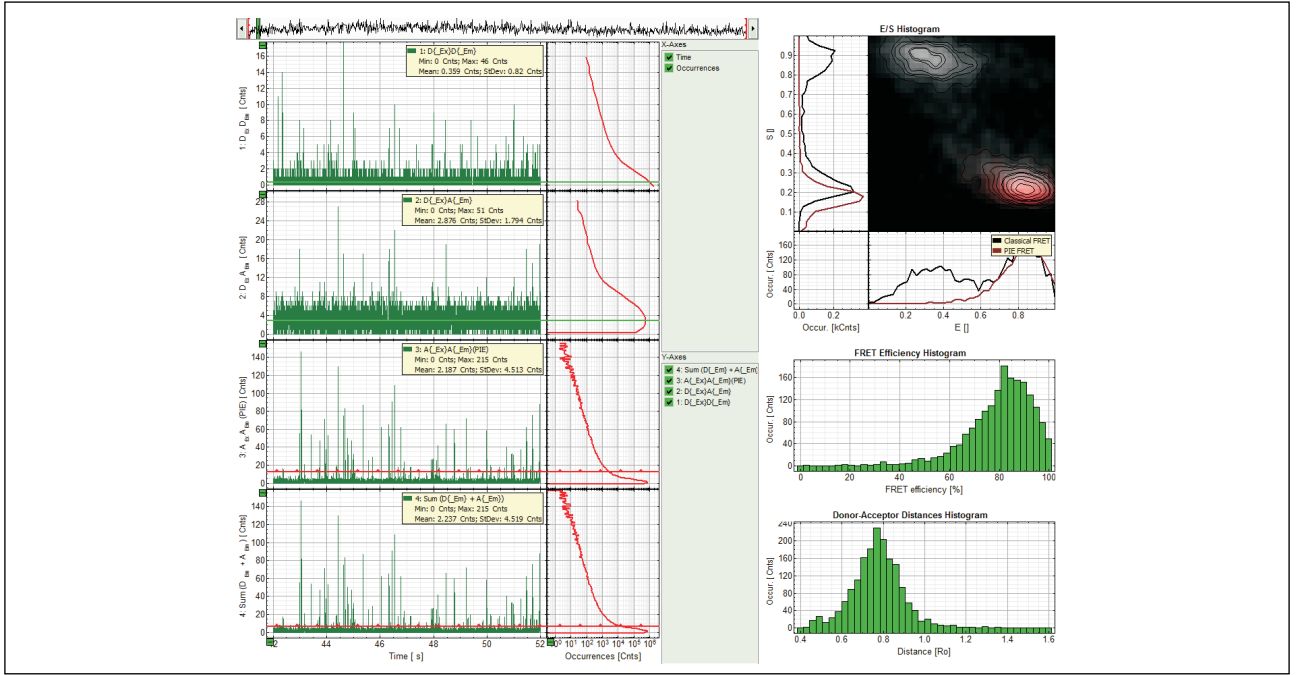


Fig. 3: Screenshot of the PIE-FRET analysis of the SymPhoTime 64 software. The four traces on the left display the intensity fluctuations over the time (see text for detailed explanation). In the E/S histogram, the FRET efficiency  $E_{FRET}$  is plotted versus the photon stoichiometry  $S_{Eff}$ . Furthermore, the PIE-FRET analysis automatically calculates the FRET efficiency histogram. Based on the FRET efficiencies, the distances between donor and acceptor are determined in values of the Förster radius  $R_0$  and displayed in the Donor-Acceptor distances histogram.

light reached the sample. The repetition frequency of each laser was set to 40 MHz. To realize the pulsed interleaved excitation with a pulse train of alternating colors, the 532 nm laser was electronically delayed by 12.5 ns with respect to the 638 nm laser. A dual band dichroic reflecting 532 nm and 638 nm guided the light to a high numerical aperture apochromatic objective (60x, NA 1.2, water immersion, Olympus), which finally focussed the light to a confocal volume of 1.1 femtoliter (resp. 1.7 femtoliter) for excitation with 532 nm (resp. 638 nm) and detection at  $(575 \pm 15)$  nm (resp.  $(685 \pm 35)$  nm). Fluorescence from excited molecules was collected with the same objective and focussed onto a 50  $\mu\text{m}$  diameter pinhole to enable confocal detection. The donor and acceptor emission was separated via a dichroic longpass filter with a dividing edge at 640 nm. Suited bandpass filters were inserted to eliminate the respective excitation wavelength and to minimize spectral crosstalk. The fluorescence was detected with two avalanche photodiodes (SPCM-AQR-14, Perkin Elmer Inc.) using Time-Correlated Single Photon Counting (TCSPC) with the TimeHarp 200 board. The data was stored in the Time-Tagged Time-Resolved Mode (TTTR), allowing to record every detected photon with its individual timing and detection channel information which is the basis for the following analysis [13]. The measurement was performed 10  $\mu\text{m}$  deep in the solution with a total acquisition time of 40 minutes.

## Results

PIE-FRET analysis is readily available in the SymPhoTime software. Fig. 3 shows a screenshot of the PIE-FRET interface. For visualization, the single photon data was summed up in bins of 1 ms, then the four channels were selected as follows (compare Fig. 1):

1. Donor trace: Detector 2 after excitation with the 532 nm laser (early time window: Ch. 64-1446)
2. Acceptor trace (this is FRET mediated acceptor emission): Detector 1 after excitation with the 532 nm laser (early time window: Ch. 64-1446)
3. PIE trace: Detector 2 after excitation with the 638 nm laser (late time window: Ch. 1450-2312)
4. Sum trace: displays all photons in the donor and acceptor channel

The third (PIE-) trace was defined as the filter channel. Only the bursts selected above the threshold indicated by the horizontal red line were further analyzed to establish the FRET histogram<sup>2</sup>.

$$E = \frac{n_A}{n_A + \gamma n_D} \quad (1)$$

<sup>2</sup> In conventional FRET analysis the sum of detector 1 (acceptor channel) and detector 2 (donor channel) after donor excitation (the acceptor is not excited directly) is used as burst-defining criterion.

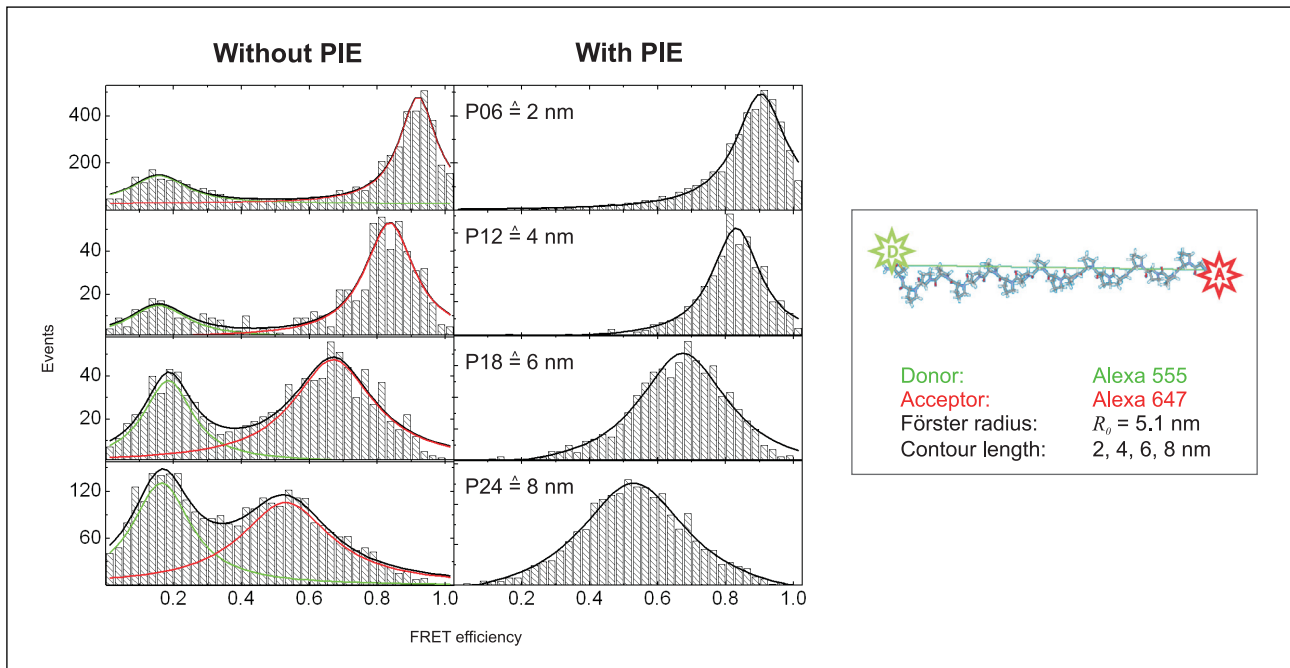


Fig. 4: Comparison of the FRET efficiencies of molecules with different polyproline ( $P$ ) numbers. Left: Conventional FRET analysis including the zero efficiency peak caused by molecules bearing only the donor fluorophore. Right: PIE-FRET analysis. The donor-only molecules, identified with additional information conveyed through PIE, causing the zero efficiency peak are excluded from the histogram.

The uncorrected FRET efficiencies  $E$  are calculated and histogrammed according to equation 1, with  $nD$  and  $nA$  being the detected numbers of photons in the bursts for the donor and acceptor channel, respectively.

Fig. 4 shows the resulting FRET distribution for different lengths of the polyproline molecules. When omitting the additional information conveyed by PIE, two peaks show up in the distribution. Only by analyzing whether an acceptor is actually present the origin of the left peak becomes apparent. The “zero efficiency” peak is caused by those polyproline molecules that miss their acceptors. Consequently, their FRET efficiency is only due to spectral crosstalk and therefore an artifact.

The PIE-FRET technique becomes even more advantageous for the study of larger FRET pair distances or the distribution of distances leading to efficiency histograms, where the two maxima do not form two distinct populations any longer.

With PIE, the three subpopulations donor-only, acceptor-only and complete FRET molecules are distinguishable and furthermore, the concentrations of all three species can be derived using time-gated FCS after burst selection. Therefore, it is in principle possible to deduce all important parameters necessary for the FRET efficiency calculation from a single measurement of a mixture containing all three subpopulations. This is of great importance under such conditions where control measurements are difficult

to perform like e.g., in living cells. For a more thorough discussion of this experiment see [14].

## Identification of populations via photon stoichiometry and FRET followed by fluorescence lifetime analysis to determine the crosstalk-free FRET efficiency

As the intensity based FRET determination suffers from various spectral crosstalk related problems that mandate calibration experiments, measuring the FRET efficiency via the FRET induced decrease of the donor fluorescence lifetime has become popular.

However, here another challenge exists since the number of photons contained in a burst produced by a single molecule is usually quite low and not sufficient for the precise determination of the FRET efficiencies. One could simply turn to the overall fluorescence lifetime in case of a homogeneous sample. This, unfortunately, is usually not possible since most samples simply are not homogeneous and therefore mandate the use of single molecule techniques.

The solution of this dilemma is to first identify the different populations in the heterogeneous sample using fluorescence intensity methods. The identified subpopulations can then be regarded as homogene-

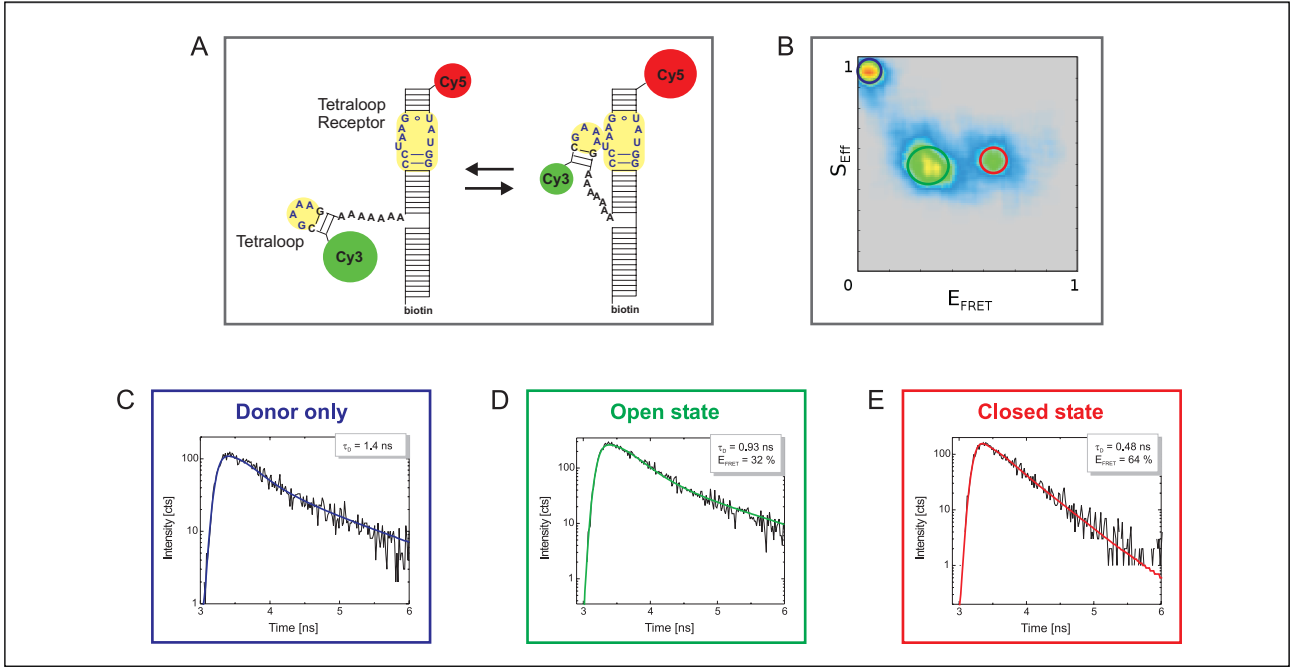


Fig. 5: Example of a RNA folding study. The trace construct containing the acceptor CY5 labeled tetraloop receptor and a flexible tetraloop fused to the donor CY3 can adopt two different conformations, a non interacting open state and a closed state where due to the interaction between tetraloop and receptor D+A are in very close proximity (A). The closed state shows FRET and therefore the donor fluorescence lifetime is reduced. Plotting the FRET efficiency  $E_{FRET}$  versus the photon stoichiometry  $S_{Eff}$ , three subpopulations were identified: molecules lacking the acceptor (blue) and intact FRET pairs in the open (green) and closed state (E). C shows the fluorescence decay for a donor-only construct while D and E display the fluorescence decay, the donor fluorescence lifetime and FRET efficiency of an intact pair in the open (D) and closed state (E).

ous among themselves and hence be analyzed as an ensemble. The statistics of these ensembles is much higher compared to one burst. Therefore, a precise determination of the FRET efficiency of the identified subpopulations is possible without the need to correct for spectral crosstalk.

Fig. 5 shows such an experiment [15]. The SymPho-Time 64 script was used to plot the intensity bursts into a 2D-histogram (Fig. 5B). The x-axis contains the FRET efficiencies as calculated by equation 1 whereas the y-axis displays the photon stoichiometry:

$$S_{Eff} = \frac{n_{A-FRET} + n_D}{n_{A-FRET} + n_D + n_{A-direct}} \quad (2)$$

The photon stoichiometry  $S_{Eff}$  is defined as the ratio of photons emitted after excitation of the donor (donor and acceptor emission channels) and the sum of all emitted photons after donor and direct acceptor excitation.

If a molecule contains only acceptor fluorophores, the denominator is zero and therefore acceptor-only molecules would have  $S_{Eff} = 0$ . Donor-only molecules on the other hand show  $S_{Eff} = 1$ . Molecules that bear both, donor and acceptor fluorophores (same brightness assumed) exhibit  $S_{Eff} = 0.5$ .

In the 2D-histogram (Fig. 5B), we can clearly distinguish three populations. The blue encircled population can be attributed to molecules that lack an acceptor fluorophore. The green and red populations are intact FRET pairs.

To calculate the FRET efficiency of those two intact populations, one uses the fluorescence lifetime of the donor of these populations (Fig. 5D and 5E) as well as the fluorescence lifetime in absence of the acceptor (Fig. 5C). All three fluorescence lifetimes are readily available from the three subpopulations.

The donor-only lifetime ( $\tau_D = 1.37$  ns) was retrieved from the blue population (Fig. 5C). Using the following equation:

$$E = \frac{\tau_{D(A)}}{\tau_D} \quad (3)$$

the FRET efficiencies of the two intact populations were calculated as indicated in Fig. 5D and 5E.

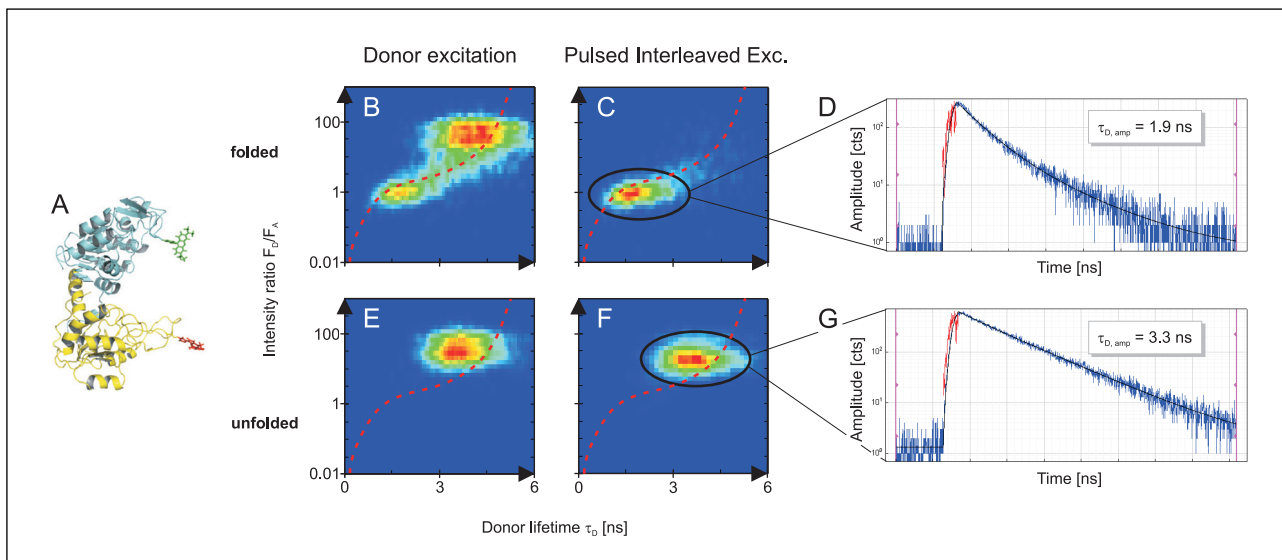


Fig. 6: Folding study of Phosphoglycerate Kinase (PGK) (A). MFD plots: donor excitation, folded (B); donor excitation, unfolded (E); PIE, folded (C); PIE unfolded (F). D and G show the fluorescence decay of the selected populations from C and F.

## Multi-Parameter Fluorescence Detection (MFD)

In this example, single-molecule FRET measurements of Phosphoglycerate Kinase (PGK) (Fig. 6) were performed at different concentrations of Guanidine Hydrochloride (GndHCl). The folding as well as the stability of this two-domain protein has been studied extensively. Since the unfolding transition of PGK by GndHCl is highly reversible at low temperature, it has become one of the model systems to study properties of multi-domain folding [33-35].

The experiments shown in this section were done in the lab of Jörg Fitter, RWTH Aachen, Germany. The experimental conditions, results and discussion have been published in [16]. We discuss here the analysis of their data using the MFD Script of the SymPhoTime Software.

The MFD script available in SymPhoTime performs an analysis based on the Multi-Parameter Fluorescence Detection (MFD) approach of single molecules as published by Claus Seidel, University of Düsseldorf, Germany [8]. It generally allows a burst-wise determination of different fluorescence parameters of single molecules in aqueous solution diffusing through the confocal volume.

In the context of this section, the script has been used to calculate the burst-wise fluorescence lifetime,  $\tau_{DA}$ , and plot it against the ratio of the donor and acceptor fluorescence,  $F_D/F_A$  into two-dimensional histograms shown in Fig. 6B, 6C, 6E and 6F.

Fig. 6B and 6E show MFD plots after direct excitation of the donor. In Fig. 6B, clearly two subpopulations

are distinguishable. One population with a low  $F_D/F_A$  ratio and a quenched donor lifetime corresponds to the high-FRET species. The other population exhibiting a high  $F_D/F_A$  ratio and an unquenched donor lifetime  $\tau_D$  represents either the low-FRET or the donor-only species. The low-FRET or donor-only population is also visible in the unfolded state (Fig. 6E). When taking the PIE information into account and by excluding all molecules with an absent acceptor (Fig. 6C and 6F), it becomes obvious that the low-FRET/donor-only population visible in Fig. 6B was caused by incompletely labeled molecules. Through PIE, the donor-only contribution can be removed and the low-FRET population can be selected for further analysis. Thus, the FRET efficiency can be derived from all measured single molecule events originating from FRET molecules and be calculated based on the enhanced statistics.

The most interesting feature of this type of MFD plot is the possibility to connect the FRET efficiency as derived from burst intensity analysis (y-axis) with the FRET efficiency derived from the burst-wise analysis of the donor fluorescence lifetime (x-axis). If the reduction of the donor fluorescence lifetime is caused by FRET, it should follow the equation:

$$\frac{F_D}{F_A} = \frac{\phi_D}{\phi_A} \frac{\tau_{D(A)}}{\tau_D - \tau_{D(A)}} \quad (4)$$

In order to facilitate the interpretation, a MatLab Script is provided to overlay the static FRET curve (eq. 4) with the 2D-histogram of  $F_D/F_A$  and  $\tau_D$ . If the position of the low-FRET for example is shifted to the left with respect to the theoretically predicted (eq. 4) position indicated by the static FRET curve (additional, non-FRET), donor quenching can be assumed.

However, a high-FRET population lying above the static FRET curve indicates acceptor quenching. Additionally, some cases of dynamic behavior can be identified. This, however, is beyond the scope of this application note. Please refer to the chapter MFD by Claus Seidel section of [8] and tutorials for the MFD-Script [17,18].

## Conclusion

The presented results clearly show that the MicroTime 200 along with its software is an extremely useful tool to investigate molecular properties and dynamics of freely diffusing molecules. FRET measurements can be employed to investigate the folding and dynamics of a wide range of biomolecules. Pulsed interleaved excitation allows for an excellent separation of different dyes due to the dye-specific excitation wavelengths, even for measurements performed in liquids (e.g., FCS). For studies resolving molecular distances in the nanometer scale, FRET can be enhanced using PIE to eliminate contributions from incomplete FRET pairs with missing or non fluorescing acceptors. The method is extendable towards excitation with more than two wavelengths for complete analysis of triple FRET as well as FRET in combination with the detection of other fluorescently labeled molecules.

### **Further applications of PIE:**

- Fluorescence Cross-Correlation (FCCS) experiments in the presence of FRET
- Enhanced sensitivity and elimination of crosstalk in FCS and FCCS experiments
- Simultaneous multicolor excitation with a single detection channel

### **Other general applications for FRET measurements include:**

- Spatial distribution and assembly of protein complexes
- Receptor/ligand interactions
- Probing interactions of single molecules
- Structure and conformation of nucleic acids
- Detection of nucleic acid hybridization
- Primer-extension assays for detecting mutations
- Automated DNA sequencing
- Distribution and transport of lipids

## References

- [1] Deniz, A. A., Dahan, M., Grunwell, J. R., Ha, T., Faulhaber, A. E., Chemla, D. S., Weiss, S., PNAS, Vol.96, p.3670-3675 (1999)
- [2] Weiss, S., Science, Vol.283, p.1676-1683 (1999)
- [3] Schuler B., Methods in Molecular Biology, Vol.350, p.115-138 (2006)
- [4] Müller B. K., Zaychikov E., Bräuchle, Ch., Lamb, D. C., Biophysical Journal, Vol.089, p.3508-3522 (2005)
- [5] Kapanidis A. N., Lee N. K., Laurence, T. A., Doose, S., Margeat, E., Weiss, S., Proceedings of the National Academy of Sciences of USA, Vol.101, p.08936-08941 (2004)
- [6] Lee N. K., Kapanidis, A. N., Wang, Y., Michalet, X., Mukhopadhyay, J., Ebright, R. H., Weiss, S., Biophysical Journal, Vol.088, p.2939-2953 (2005)
- [7] Laurence, T. A., Kong, X., Jäger, M., Weiss, S., Proceedings of the National Academy of Sciences of USA, Vol.102, p.17348-17353 (2005)
- [8] Sisamakias, E., Valeri, A., Kalinin, S., Rothwelllow, P. J., Seidel, C. A. M., Methods in Enzymology, Vol.475, p.455-514 (2010)
- [9] Wahl, M., Koberling, F., Patting, M., Rahn, H.-J., Erdmann, R., Curr. Pharm. Biotech., Vol.5, p.299-308 (2004)
- [10] Stryer, L., Haugland, R. P., Proc. Natl. Acad. Sci., USA 58, Vol.2, p.719-726 (1967)
- [11] Schuler, B., Lipman, E. A., Eaton, W. A., Nature, Vol.419, p.743-747 (2002)
- [12] <http://probes.invitrogen.com/handbook/tables/1570.html>
- [13] Wahl, M., Erdmann, R., Lauritsen, K., Rahn, H.-J., Proc. SPIE, Vol.3259, p.173-178 (1998)
- [14] Ruettinger S., Macdonald R., Kraemer B., Koberling F., Roos M., Hildt E., Journal of Biomedical Optics, Vol.11, 024012 (2006)
- [15] Fiore, J. L., Kraemer, B., Koberling, F., Erdmann, R., Nesbitt, D. J., Biochemistry, Vol.48, p.02550-02558 (2009)
- [16] Rosenkranz, T., Schlesinger, R., Gabba, M., Fitter, J., ChemPhysChem, Vol.12, p.0704-0710 (2011)
- [17] [http://www.picoquant.com/technotes/Tutorial\\_MFD\\_02.pdf](http://www.picoquant.com/technotes/Tutorial_MFD_02.pdf)
- [18] [http://www.picoquant.com/technotes/Tutorial\\_MatlabscriptMFD.pdf](http://www.picoquant.com/technotes/Tutorial_MatlabscriptMFD.pdf)



PicoQuant GmbH  
Rudower Chaussee 29 (IGZ)  
12489 Berlin  
Germany

Phone +49-(0)30-6392-6929  
Fax +49-(0)30-6392-6561  
Email [info@picoquant.com](mailto:info@picoquant.com)  
WWW <http://www.picoquant.com>

Copyright of this document belongs to PicoQuant GmbH. No parts of it may be reproduced, translated or transferred to third parties without written permission of PicoQuant GmbH. All Information given here is reliable to our best knowledge. However, no responsibility is assumed for possible inaccuracies or omissions. Specifications and external appearances are subject to change without notice.

© PicoQuant GmbH, 2013